COMMUNICATIONS IN SCIENCE AND TECHNOLOGY
Homepage: cst.kipmi.or.id

Rice husk ash-based selective absorbent with imprinted ionic for gold recovery

Sri Hastuti*, Ema N. Fajariani, Intan K. Candraningrum, Tri Martini, Sayekti Wahyuningsih, Fitri N. Aini

Department of Chemistry, Universitas Sebelas Maret, Surakarta 57126, Indonesia

Article history:
Received: 19 June 2024 / Received in revised form: 8 September 2024 / Accepted: 7 October 2024

Abstract

The recovery of gold from aqueous solutions is crucial due to its economic value and environmental significance, making effective separation technologies essential. To tackle this challenge, development of an adsorbent with enhanced selectivity and high adsorption capacity against Au(III) is highly crucial. This present study harnessed rice husk derived-silica functionalized by (3-trimethoxysilyl)propyldiethylenetriamine (TMPDT) using imprinted ionic method to form SiO_2-TMPDT-Au-Imp, specifically designed for the selective adsorption of Au(III). SiO_2-TMPDT-Au-Imp demonstrated a significantly higher adsorption capacity about 387% improvement compared to SiO_2-TMPDT, highlighting its superior performance. Furthermore, in addition to exhibit several advantageous characteristics that surpass those of other materials tested, underscoring its effectiveness in Au(III) adsorption. SiO_2-TMPDT-Au-Imp displayed notable selectivity in competitive metal ion solutions with the preference order of Au(III)/Fe(III) < Au(III)/Cu(II) < Au(III)/Zn(II). The developed SiO_2-TMPDT-Au-Imp, in brief, represents a promising advancement in the field of material science and environmental remediation in which it offers a tailored solution for efficient and selective adsorption of Au(III). This study can also be applied for the recovery of Au(III) ions from electronic waste.

Keywords: Silica; Rice husk ash; adsorbent; ionic-imprinted materials

1. Introduction

Over the past few decades, the demand for precious metals such as gold has surged, driven by their essential roles in industrial processes and jewellery market. This increasing demand, coupled with the gradual depletion of high-grade ore resources and the enforcement of stricter environmental regulations, has made the development of efficient and sustainable extraction technologies a critical priority. On the other side, electronic and industrial waste have emerged as valuable secondary sources for precious metals, prompting the exploration of various recovery methods [1]. Techniques such as ion exchange [2], chemical precipitation [3], electrochemistry [4], complexation, and solvent extraction [5] have been employed, but adsorption has garnered a significant attention in view of its low cost, simplicity, and efficiency in an industrial scale [1]. Efforts to produce effective adsorbents have led to the use of both natural and synthetic materials, including activated carbon [6], zeolite [7], chitosan [8], and silica [9]. Of these, silica (SiO_2) has proven to be particularly promising for water remediation applications as it is environmentally friendly, resistant to acidity, cost-effective, and easily modifiable [10]. The combination of these favourable properties makes silica a strong candidate for advancing the sustainable recovery of precious metals from waste streams, addressing both economic and environmental challenges.

Silica is a versatile material that can be sourced from a variety of natural resources. Rice husk is one particularly rich source of silica, containing about 15-20% silica; even this percentage can reach approximately 89.47–98% in rice hull ash (RHA). Compared to other agricultural by-products like bagasse fly ash, rice husks are notable for their higher density, attributed to their substantial silica content [11]. The silica obtained from rice husk has a high surface area and porosity, making it resistant to chemical and microbial degradation [12]. The intrinsic functional groups in silica, such as silanol (-Si-OH) and siloxane (-Si-O-Si), allow it to adsorb heavy metals. This natural adsorption capability, nevertheless, possesses some limitations such as the frequently irreversible binding process to metal ions and the low selectivity for specific metals.

* Corresponding author.
Email: srihastuti71@staff.uns.ac.id
https://doi.org/10.21924/cst.9.2.2024.1461

To overcome these challenges, the active sites on silica can be modified by means of organosilane or organic compounds to enhance its effectiveness as an adsorbent.

Researchers have explored various modifiers to improve the performance of silica in heavy metal adsorption. Ethylenediamine triacetic acid (EDTA) [13], 3-aminopropyltrimethoxysilane (APTMS) [14], and N-(3-trimethoxysilyl)propyldiethylenetriamine (TMPDT) [15], for instance, have been used to functionalize silica. Of these, TMPDT is deemed particularly effective due to its three amine groups, which can be protonated to form ammonium ions. This property significantly enhances its ability to bind heavy metal ions, such as Au(III). Moreover, the development of ionic imprinted techniques has further advanced the capability of modified silica in selectively removing heavy metals from various environments. These techniques have been successfully applied to target and remove metals such as cadmium Cd^{2+}) [16], copper Cu^{2+}[17,18], silver (Ag^{+}) [19], mercury (Hg^{2+}) [20], and gold (Au^{3+}) [1,11,21–23] ions from complex mixtures. The primary advantage of the imprinted ion synthesis technique is its ability to create highly selective adsorption sites by forming porous networks with varying pore sizes and diverse chemical functionalities, which can be customized to meet the specific needs of different applications [1]. When metal ions are imprinted and subsequently removed from the silica structure, they leave behind the cavities of specific shapes and sizes. These cavities are perfectly suited for re-binding the same type of metal ions, thus enhancing the selectivity and efficiency of the adsorption process. The imprinted ionic technique effectively transforms the silica into a highly selective adsorbent tailored for the target metal ions.

In this study, we explored the potential of rice husk-derived silica as a sustainable and efficient source for fabricating a selective Au(III) adsorbent, SiO_2–TMPDT-Au-Imp. The use of silica derived from rice husk ash is still relatively uncommon. While rice husk ash offers a sustainable and cost-effective alternative, it has not been widely adopted in certain advanced applications [16–18,24]. In contrast, more conventional silica sources, such as tetraethyl orthosilicate (TEOS), are frequently employed, particularly in specialized processes like the synthesis of imprinted ionic materials. TEOS is a well-established precursor in these applications, offering consistent and reliable results, which may explain why it remains the preferred choice over less conventional sources like rice husk ash. However, the potential of rice husk ash as a silica source remains largely untapped but could be explored further for its environmental and economic benefits. By comparing its performance with other materials, we demonstrated that this modified silica not only has a high capacity for Au(III) adsorption but also exhibits superior selectivity.

2. Materials and Methods

2.1. Materials

The materials used in this research include rice husk, which was collected from a local market in Surakarta. Chemical reagents such as thiourea, sodium hydroxide (NaOH), nitric acid (HNO_3), and 37% hydrochloric acid (HCl) were obtained from Merck. N-(3-trimethoxysilyl)propyldiethylenetriamine (TMPDT) was purchased from Sigma Aldrich. $HAuCl_4$ (1000 mg/L) solution, used as the source of Au(III) ions, was supplied by the Analytical Laboratory of Universitas Gadjah Mada. Additionally, high-purity gold was acquired from a jewellery boutique used to prepare the gold solution standard by dissolving in aquaregia (a mixture of HCl and HNO_3 with a composition ratio of 3:1).

2.2. Preparation of Au(III) ion-imprinted SiO_2 derived from Rice husk ash (SiO_2-TMPDT-Au-Imp)

SiO_2-TMPDT-Au-Imp was prepared using an improved procedure based on the method reported by Sakti et al [11]. The first step to prepare this material was synthesis of Na_2SiO_3 from Rice husk ash. Briefly, the Rice husk ash (RHA, 20 g) was immersed with 160 mL of 4 M NaOH and boiled until a thick suspension formed. Afterward, the gel was then calcined at 500 °C for 30 minutes. The resulting powder was soaked in distilled water for 24 hours to obtain Na_2SiO_3. After confirming the Na_2SiO_3 product, the SiO_2-TMPDT-Au-Imp was then prepared in the second step. About 100 mL of Na_2SiO_3 was mixed with 5 mL of TMPDT and 5 mL of Au(III) solution (1000 mg/L), followed by the addition of 6 M HCl dropwise until pH 7. The precipitate was collected and dried at 70 °C. The dried gel was milled to pass through a 200-mesh sieve. The gold content in the dried gel was then released using a 7% thiourea in HCl 1M solution, resulting in the SiO_2-TMPDT-Au-Imp adsorbent material. This material was subsequently characterized using Fourier-transform infrared spectroscopy (FTIR), thermogravimetric analysis (TGA), and specific surface area analysis (SAA).

2.3. Study of pH effect on Au(III) adsorption

The impact of pH on the adsorption process was studied by introducing 10 mg of adsorbent into 10 mL of a 15 mg/L Au(III) solution at different pH levels. The mixture was agitated at 120 rpm for one hour at room temperature, followed by filtration through Whatman filter paper to obtain the filtrate for analysing the remaining Au(III) content.

2.4. Kinetic and isotherm adsorption study

To investigate the adsorption kinetics, 10 mg of the adsorbent was added to 10 mL of a 90 ppm Au(III) solution at the optimum pH. The mixture was shaken at different contact times to observe the adsorption rate, and subsequently filtered using Whatman filter paper to separate the adsorbent from the solution.

For the adsorption isotherms study, 10 mg of the adsorbent was contacted with 10 mL of Au(III) solutions of varying concentrations (0, 10, 20, 30, 40, 60, 80, and 100 mg/L) at the optimum pH and contact time. This allowed the evaluation of how different concentrations of Au(III) influenced the adsorption capacity of the adsorbent.

To examine the selectivity of the adsorbent, a multi-metallic solution containing Cu(II), Zn(II), and Fe(III) at concentrations of 5, 10, and 15 mg/L was prepared. In each experiment, 10 mg of the adsorbent was mixed with 10 mL of a solution containing 100 mg/L of Au(III) and one of the other metal ions. This setup

was used to assess the adsorbent's preference for Au(III) in the presence of competing metal ions.

3. Results and Discussion

Fig. 1 illustrates the formation process of SiO_2-TMPTD-Au-Imp for the selective adsorption of Au(III)[16–18,25,26]. Initially, $(SiO_3)^{2-}$ ions reacted with hydrogen from H_2O and HCl, resulting in the formation of $Si(OH)_4$. Simultaneously, the amine group (NH_2) of TMPDT underwent protonation to produce an ammonium group (NH_3^+). This protonated ammonium group effectively bound Au(III) ions through electrostatic interactions. Upon the addition of HCl, the Si-OCH_3 bonds in the silane compound became unstable and this led to the protonation of silicon and the subsequent release of methoxy groups (-OCH_3), combining H^+ to form methanol (CH_3OH) as a by-product. The resulted electropositive silicon atoms then bound OH^- ions. Following this, condensation and polymerization processes occurred. In these processes, $Si(OH)_4$ produced from the initial reaction interacted with TMPDT-Au(III), leading to the release of H_2O molecules and the formation of a solid gel. This gel consisted of elongated polymer chains. The Au(III) metal ions attached to the active sites of TMPDT were desorbed, forming specific cavities within the structure that acted as templates for Au(III) metal ions, leading to the creation of SiO2-TMPDT-Au-Imp. Finally, when the SiO_2-TMPDT-Au-Imp material was exposed to Au(III) solution, $AuCl_4^-$ ions occupied the specific active sites within the pores of the material, demonstrating the targeted adsorption capability of the modified silica.

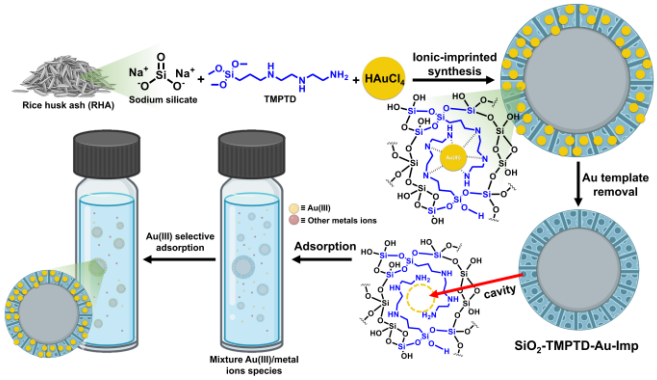

Fig. 1. Schematic illustration of the synthesis SiO_2-TMPTD-Au-Imp from rice husk ash for selectively adsorbing the gold ions

3.1. Characteristics of SiO_2-TMPDT-Au-Imp

Fig. 2 illustrates the FTIR spectrum of SiO_2 derived from rice husk. The spectrum revealed a broad peak at 3443 cm^{-1}, which corresponded to the stretching vibrations of hydroxyl (−OH) and silanol (Si−OH) groups. This observation aligned with the findings of a study by Priya et al. [27]. Additionally, a peak at 1642 cm^{-1} was attributed to the bending vibrations of water molecules present in the silica structure. The prominent peak at 1089 cm^{-1} is the indicative of the asymmetric stretching vibrations of siloxane (Si−O−Si) groups, confirming the presence of these functional groups in the silica matrix. Furthermore, symmetric stretching vibrations of Si−O bonds were observed at 795 cm^{-1}. The FTIR spectrum of the synthesized ionic imprinted material, SiO_2-TMPDT-Au-Imp, revealed similar characteristic peaks to those of SiO_2, indicating that the basic silica structure was retained after being modified. However, a notable difference was found in the appearance of a new peak in the range of 1650 cm^{-1}. This peak was associated with the N−H bending vibrations, suggesting the successful incorporation of TMPDT into the silica matrix. The presence of the N−H group confirmed that TMPDT has been effectively bound to the SiO_2-TMPDT-Au-Imp material, enhancing its functionality for specific adsorption applications. These spectral features demonstrated that the synthesized SiO_2-TMPDT-Au-Imp retained several essential characteristics of the original SiO_2 while incorporating additional functional groups from TMPDT.

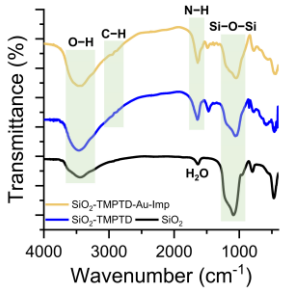

Fig. 2. FTIR spectrum of SiO_2 synthesized from RHA, SiO_2-TMPDT, and SiO_2-TMPDT-Au-Imp

Table 1 provides a summary of the surface area and pore characteristics of the adsorbents. Measuring these properties was deemed essential for ionic imprinted materials as they directly influenced the adsorption capacity and efficiency of the adsorbents. The SiO_2-TMPDT-Au-Imp adsorbent exhibited a reduced surface area of 21.136 m^2/g compared to SiO_2 as reported in previous research [11]. This reduction in surface area was likely due to the coverage of the silica surface by modifier groups (TMPDT), occupying the surface sites. Additionally, the decrease in pore volume for SiO_2-TMPDT-Au-Imp could be attributed to the formation of the Au imprinted structure within the pores, which partially filled the pore space. The imprinting process also caused a shift in the average pore radius to a larger size, indicating that the modification altered the pore structure. While surface area, pore volume, and pore diameter are the important factors in determination of the adsorption capacity, they are not the sole indicators of adsorption performance. The presence and accessibility of active sites on the surface of the adsorbent are also critical for effective adsorption. Therefore, while the physical properties provide valuable insights, the chemical functionality imparted by the TMPDT modification plays a significant role in enhancing the material's adsorption capabilities for gold ions.

Table 1. Surface area and porosity of SiO_2-TMPDT, SiO_2-TMPDT-Au and SiO_2-TMPDT-Au-Imp

Absorbent	Surface area (m^2/g)	Volume of pores (cc/g)	Pore radius (Å)
SiO2-TMPDT	54.679	0.170	19.193
SiO2-TMPDT-Au	31.214	0.081	28.724
SiO2-TMPDT-Au-Imp	21.136	0.043	21.673

The thermal stability of SiO_2-TMPDT-Au-Imp was assessed through thermogravimetric analysis (TG) and differential thermal analysis (DTA), as shown in Fig. 3. The analysis revealed that the first significant mass reduction occurred at the temperatures of 125.90°C, 148.80°C, and 116.80°C, corresponding to a mass loss of 14.43%, 17.21%, and 11.81% for SiO_2-TMPDT-Au, SiO_2-TMPDT, and SiO_2-TMPDT-Au-Imp, respectively. This initial mass loss was primarily attributed to the release of physically adsorbed water molecules. The second phase of mass reduction was observed due to the release of water from the condensation of silanol groups (Si-OH) to form siloxane bonds (Si-O-Si). This step indicated further dehydration and stabilization of the silica network. Additionally, the final reduction phase was associated with the decomposition and release of organic compounds and the condensation of any remaining silanol groups. This step marked the completion of the thermal transformation processes within the material [28]. The release of organic molecules from SiO_2-TMPDT-Au-Imp was found greater compared to SiO_2-TMPDT-Au and SiO_2-TMPDT with the mass losses of 66.01%, 13.07%, and 10.57%, respectively. This significant weight loss was attributed to the desorption of Au ions, which served as a template in the imprinted material. The higher mass loss indicated a greater presence of organic molecules and confirmed the successful incorporation and subsequent release of Au ions from the imprinted adsorbent.

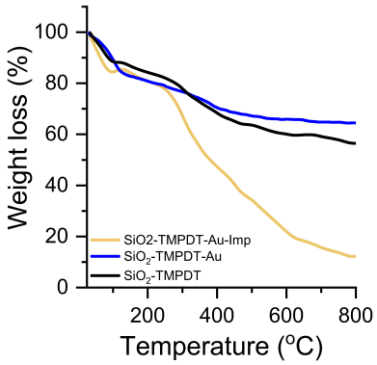

Fig. 3. TGA curve of SiO_2-TMPDT, SiO_2-TMPDT-Au, and SiO_2-TMPDT-Au-Imp

3.2. Effect of pH toward the Au(III) adsorption onto SiO_2-TMPDT-Au-Imp

The pH of the metal ion solution is a crucial factor in adsorption as it greatly affects the ability of the adsorbent material to bind the target metal ions [29]. The impact of pH on the adsorption of Au(III) was examined across a pH range of 1, 2, 3, 4, 5, and 6, as depicted in Fig. 4. Both SiO_2-TMPDT and SiO_2-TMPDT-Au-Imp showed a decrease in adsorption capacity along with the decreasing pH with the optimum pH identified as 3. At low pH levels (1 and 2), the high concentration of H^+ ions significantly impacted the adsorption process. The H^+ ions reacted with $AuCl_4^-$ anions to form $HAuCl_4$, which is a neutral molecule. This neutralization reduced the availability of Au(III) ions for binding, thus decreasing the adsorption capacity of the adsorbent.

Furthermore, at these low pH levels, functional groups such as amine groups (-NH-) present on the adsorbent surface became protonated to form $-NH_3^+$ groups. This protonation reduced the number of active sites available for binding Au(III) ions, leading to a further decline in adsorption efficiency [29]. Conversely, at higher pH levels (4, 5 and 6), the adsorption capacity also decreased, but for different reasons. As the pH increased, the concentration of chloride ions (Cl^-) in the solution decreased. These Cl^- ions are essential to form the R-$NH_3^+AuCl_4^-$ complex, which facilitates the binding of Au(III) ions to the adsorbent. When there are fewer Cl^- ions available, the formation of this complex is hindered, thereby reducing the adsorption capacity [30].

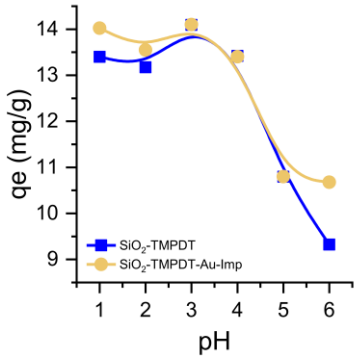

Fig. 4. The influence of pH on the Au(III) adsorption capacity of SiO2-TMPDT-Au-Imp and SiO2-TMPDT

3.3. Study of adsorption kinetics

The rate and time required to reach equilibrium in the uptake of metal ions are described by adsorption kinetics, which provide insights into the efficiency and mechanism of the adsorption process. Fig. 5 reveals the relationship between adsorption time and the adsorption capacity of Au(III). The data indicated that equilibrium was reached within 30 minutes, suggesting a rapid adsorption process. To further understand the kinetics of Au(III) adsorption, several models were employed, including first-order, second-order, pseudo-first-order, and pseudo-second-order equations. These models helped to determine the mechanism and rate-controlling steps of the adsorption process. Of the tested models, the pseudo-second-order kinetic model exhibited the highest correlation coefficient (R^2), implying a better fit to the experimental data.

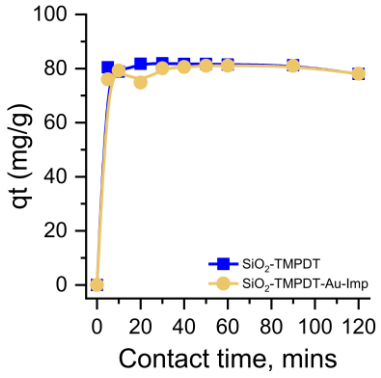

Fig. 5. The relationship between contact time and adsorption capacity of Au(III) within SiO_2-TMPDT and SiO_2-TMPDT-Au-Imp

The equilibrium adsorption capacity obtained

experimentally (qe_{exp}) was observed to closely match the calculated adsorption capacity (qe_{cal}), as shown in Table 2. This indicated that the processes of adsorption kinetic aligned well with the pseudo-second-order model. The consistency between qe_{exp} and qe_{cal} suggested that the adsorption mechanism was predominantly controlled by chemisorption, involving valence forces through the sharing or exchange of electrons between the adsorbent and Au(III) ions. This finding reinforces the conclusion that the pseudo-second-order model accurately describes the kinetics of Au(III) adsorption onto the modified SiO_2-TMPDT-Au-Imp material, providing a robust framework for predicting the adsorption behaviour and optimizing the adsorbent's performance in practical applications.

Table 2. Kinetics parameters for Au(III) adsorption onto SiO_2-TMPDT and SiO_2-TMPDT-Au-Imp

Kinetic model		SiO_2-TMPDT	SiO_2-TMPDT-Au-Imp
Pseudo-First Order	qe_{cal} (mg/g)	3.05	5.17
	k (min^{-1})	0.01	0.03
	R^2	0,13	0.25
Pseudo-Second Order	qe_{cal} (mg/g)	83.33	83.33
	k (mM^{-1} min^{-1})	-0,01	-0.07
	R^2	0.99	0.99
	*qe_{exp}	81.43	81.07

3.4. Effect of Au(III) concentration on adsorption ability

As shown in Fig. 6, the effect of Au(III) metal ion solution concentration on the adsorption capacity of SiO_2-TMPDT and SiO_2-TMPDT-Au-Imp was investigated by plotting the curve between variations in metal ion concentration and absorbance. The results indicated that the adsorption capacity of SiO_2-TMPDT-Au-Imp was superior compared to SiO_2-TMPDT. This enhanced performance could be attributed to the increased number of active sites and the pore structure of the SiO_2-TMPDT-Au-Imp material, which were particularly well-suited for the adsorption of Au(III) metal ions.

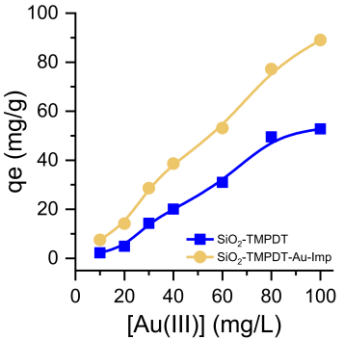

Fig. 6. The influence of Au(III) concentration on the adsorption ability of SiO_2-TMPDT and SiO_2-TMPDT-Au-Imp

3.5. Study of adsorption isotherm

The adsorption isotherm models of Au(III) were evaluated using both the Langmuir and Freundlich models to understand the adsorption mechanisms better. Table 3 presents the summarized results of these models. In the Langmuir model, Qm represents the maximum adsorption capacity, and KL is the Langmuir isotherm constant, while the Freundlich model uses KF to denote the isotherm constant, reflecting the adsorption capacity of the adsorbent. The Langmuir model suggests that the adsorption process involves physical interactions and occurs on a homogeneous surface where Au(III) ions form a monolayer on the adsorbent. This implies that each adsorption site can hold only one Au(III) ion and that all sites are energetically equivalent [29,31]. Meanwhile, the Freundlich model represents multilayer adsorption, indicating that Au(III) metal ions are adsorbed on heterogeneous surfaces and within pores, achieving maximum adsorption capacity.

Table 3. Langmuir and Freundlich isotherm parameter for Au(III) metal ion adsorption onto SiO_2-TMPDT and SiO_2-TMPDT-Au-Imp

Isotherm parameter	Adsorbent	
	SiO_2-TMPDT	SiO_2-TMPDT-Au-Imp
Langmuir:		
Qm (mg/g)	17.99	87.69
KL (g/mol)	4736.50	82293.04
RL	0.81	0.19
R^2	0.72	0.37
ΔG (kJ/mol)	21.11	28.23
Freundlich:		
KF (mg/g)	1301.86	130156.60
N	0.56	0.70
R^2	0.98	0.93

The correlation coefficient (R^2) for the Freundlich model was found higher than that of the Langmuir model, indicating that the adsorption of Au(III) onto SiO_2-TMPDT-Au-Imp was better as described by multilayer adsorption. The Freundlich model suggested a chemical interaction between Au(III) ions and the adsorbent, involving electrostatic forces. Under acidic conditions, the positively charged NH_3^+ groups attracted the negatively charged $AuCl_4^-$ ions. This interaction occurred through the silanol (Si-OH) and siloxane (Si-O-Si) groups on the adsorbent. The interaction between the gold chloride complex and the positively charged centres further supported the multilayer adsorption mechanism [1].

The comparative analysis of N value clearly showed that SiO_2-TMPDT-Au-Imp had a significantly higher adsorption capacity for Au(III) ions than that of SiO_2-TMPDT. Specifically, adsorption in SiO_2-TMPDT-Au-Imp occurred at the active sites within the pores and through the imprinted cavities, demonstrating a higher efficiency (70% compared to 56%). This indicated the crucial role of the imprinted cavities in enhancing the adsorption capacity.

Furthermore, the Gibbs free energy (ΔG) values for the adsorption processes were calculated to be 21.11 kJ/mol for SiO_2-TMPDT and 28.23 kJ/mol for SiO_2-TMPDT-Au-Imp. Given that Gibbs free energy values for chemical bonds are generally ≥ 20 kJ/mol, these results suggested that the

interactions between the adsorbents and Au(III) ions involve significant chemical interactions. The higher Gibbs free energy for SiO_2-TMPDT-Au-Imp indicated a stronger and more favourable adsorption process compared to SiO_2-TMPDT.

The adsorption capacity of SiO2-TMPDT-Au-Imp, in comparison to other adsorbents, is summarized in Table 4. These results clearly indicate that the adsorption capacity of Au(III) ions on SiO2-TMPDT-Au-Imp is substantially greater than that of other reported adsorbents, emphasizing the excellent performance of the newly developed material.

This significant increase in adsorption capacity can be attributed to the large number of active sites and the pore structure tailored for Au(III) ions. Therefore, SiO_2-TMPDT-Au-Imp stands out as a highly efficient adsorbent for gold recovery, surpassing the performance of previously reported materials.

Table 4. Adsorption capacity of Au(III) on various reported adsorbents

Adsorbents	BET Surface area (m^2/g)	Pore volume (cm^3/g)	Pore diameter (nm)	Qm (mg/g)	Ref.
coP-TEDMA/ EGDMA	58	0.22	15.1	22.20	[32]
Ionic imprinted amino-silica hybrid (Im-ASH)	143.68	1.04	157.52	76.14	[11]
TiO_2 immobilized on silica gel	NA	NA	NA	3.56	[33]
3-(8-Quinolinylazo)-4-hydroxybenzoic acid modified nano-sized alumina	NA	NA	NA	17.70	[34]
SiO_2-TMPDT	54.67	0.17	19.193	17.99	This work
SiO_2-TMPDT-Au-Imp	21.13	0.043	21.67	87.69	This work

3.6. Selectivity adsorption study of Au(III) onto SiO_2-TMPDT-Au-Imp

The adsorption selectivity of Au(III) was evaluated using the adsorption coefficient (α) in the presence of Fe(III), Cu(II), and Zn(II), as presented in Table 5. A higher selectivity coefficient indicated that the adsorbent was more selective towards Au(III). If the adsorption selectivity for Au(III) was high, the interference from competing metal ions like Fe(III), Cu(II), and Zn(II) diminished, and conversely, if the selectivity was low, the competition increased. The data demonstrated that SiO_2-TMPDT-Au-Imp had significantly higher selectivity for Au(III) compared to SiO_2-TMPDT, especially in the presence of Zn(II). This high selectivity was attributed to the specific interactions between the Au(III) ions and the functional groups on the adsorbent, as well as the entrapment of Au(III) within the imprinted cavities.

In aqueous solutions, Fe(III), Cu(II), and Zn(II) form hydrated metal complexes such as $[Fe(H_2O)_6]^{3+}$, $[Cu(H_2O)_6]^{2+}$, and $[Zn(H_2O)_6]^{2+}$. These complexes interact with the silanol (Si-OH) and siloxane (Si-O-Si) groups of the adsorbent through hydrogen bonding. Specifically, the H_2O ligands on these metal ions can form hydrogen bonds with the silanol groups on the adsorbent surfaces, leading to potential competition for binding sites. On the other hand, the interaction between the adsorbent and Au(III) metal ions is influenced by both electrostatic and chemical interactions. The electrostatic attraction occurs between the positively charged NH_3^+ groups on the adsorbent and the negatively charged $AuCl_4^-$ ions. Additionally, the Au(III) ions are trapped within the pores of the adsorbent, particularly within the imprinted cavities, enhancing the adsorption process. Accordingly, the selectivity order of metal ions on SiO_2-TMPDT-Au-Imp adsorbents is as follows: Au(III)/Fe(III) < Au(III)/Cu(II) < Au(III)/Zn(II). These findings are consistent with the research conducted by Hastuti et al. [12], which also highlighted the superior selectivity of Au(III) over other metal ions.

Table 5. Adsorption selectivity of Au(III) metal ion onto SiO_2-TMPDT and SiO_2-TMPDT-Au-Imp with the presence of metal ion interferences

Metal solution	Cons. (mg/L)	Selectivity coefficient (α)	
		SiO_2-TMPDT	SiO_2-TMPDT-Au-Imp
Au(III)-Fe(III)	5	0.11	9.14
	10	0.56	8.51
	15	0.31	10.66
Au(III)-Cu(II)	5	0.16	10.93
	10	0.14	25.32
	15	0.18	139.87
Au(III)-Zn(II)	5	1.02	6112.90
	10	0.98	872.16
Au(III)-Fe(III)	15	1.60	436.93

3.7. Desorption

As shown in Table 6, it was observed that as desorption time increased, the amount of Au(III) ions being desorbed decreased. This reduction in desorption efficiency over time was likely due to a re-adsorption phenomenon, where the Au(III) ions that were initially desorbed from the adsorbent re-interacted with the surface of the adsorbent. As the desorption process progressed, the Au(III) ions, instead of remaining in the solution, may return to contact with the active sites on the adsorbent. These active sites have a strong affinity for Au(III) ions, leading to a re-attachment of the ions onto the adsorbent's surface.

Table 6. Desorption study of Au(III) from the SiO_2-TMPDT and SiO_2-TMPDT-Au-Imp

Desorption time (mins)	SiO_2-TMPDT (mg/L)	SiO_2-TMPDT-Au-Imp (mg/L)
60	32.45	82.75
90	47.09	70.01
150	51.30	50.35
200	46.96	62.01

Additionally, during this interaction, it is suspected that the

Au(III) ions undergo a reduction reaction at the active sites where they are converted from their ionic form (Au^{3+}) to elemental gold (Au^0), possibly in the form of nanoparticles [1,35] This reduction to Au^0 is significant because it suggests that the adsorbent not only captures and holds Au(III) ions but also facilitate their transformation into a more stable and valuable form gold nanoparticles. Over time, as more Au(III) ions are reduced and accumulate as Au^0 on the adsorbent, the efficiency of desorption diminishes, leading to the observed decrease in desorption with prolonged time.

4. Conclusion

The SiO_2-TMPDT-Au-Imp adsorbent was synthesized using a combination of the ionic imprinted technique and sol-gel process where Na_2SiO_3 derived from RHA served as the precursor, TMPDT acted as the modifier compound, and Au(III) metal ion acted as the template. The adsorption isotherm models (Langmuir and Freundlich) provided insights into the adsorption behaviour of Au(III) ions on SiO_2-TMPDT-Au-Imp. The Freundlich model, which accounts for multilayer adsorption on heterogeneous surfaces, fitted the experimental data better than the Langmuir model, indicating that Au(III) ions were adsorbed through multiple layers and interactions on the adsorbent surface. The adsorption capacity of Au(III) ions by SiO_2-TMPDT-Au-Imp was notably higher compared to SiO_2-TMPDT and other reported adsorbents. This higher capacity underscored the efficiency of SiO_2(RHA)-TMPDT-Au-Imp for gold recovery applications. Furthermore, the adsorption selectivity coefficient (α) analysis demonstrated that SiO_2-TMPDT-Au-Imp exhibited high selectivity for Au(III) ions over interfering metal ions (Fe(III), Cu(II), Zn(II)). This selectivity was attributed to specific interactions, including electrostatic attraction and complex formation between Au(III) ions and the functional groups on the adsorbent surface. Therefore, SiO_2-TMPDT-Au-Imp is a promising adsorbent material with high efficiency and selectivity for Au(III) ion adsorption. Its application in gold recovery processes could offer significant advantages in terms of both adsorption capacity and selectivity, contributing to environmental remediation and resource recovery efforts. In future, the IMP for Au(III) extraction from electronic waste should focus on optimizing imprinting conditions and developing high-performance materials to improve selectivity and capacity. Efforts should also be made to scale up the synthesis for practical applications and assess the durability, reusability, and economic feasibility of the polymers. Integrating IMPs with existing recycling technologies and evaluating their environmental impact will further enhance the efficiency and sustainability of Au(III) recovery processes.

Acknowledgements

The authors would like to acknowledge Universitas Sebelas Maret for funding through fundamental research grants (No:543/UN27.21/PP/2018).

References

1. X. Gao, J. Liu, M. Li, C. Guo, H. Long, Y. Zhang, L. Xin, *Mechanistic study of selective adsorption and reduction of Au (III) to gold nanoparticles by ion-imprinted porous alginate microspheres*, Chem. Eng. J. 385 (2020) 123897.
2. A. Bashir, L.A. Malik, S. Ahad, T. Manzoor, M.A. Bhat, G.N. Dar, A.H. Pandith, *Removal of Heavy Metal Ions from Aqueous System by Ion-Exchange and Biosorption Methods*, Environ. Chem. Lett. 17 (2019) 729–754.
3. Y. Zhang, X. Duan, *Chemical Precipitation of Heavy Metals from Wastewater by Using The Synthetical Magnesium Hydroxy Carbonate*, Water. Sci. Technol. 81 (2020) 1130–1136.
4. J. Du, T.D. Waite, P.M. Biesheuvel, W. Tang, *Recent advances and prospects in electrochemical coupling technologies for metal recovery from water*, J. Hazard. Mater. 442 (2023) 130023.
5. S. Dhiman, B. Gupta, *Partition studies on cobalt and recycling of valuable metals from waste Li-ion batteries via solvent extraction and chemical precipitation*, J. Clean. Prod. 225 (2019) 820–832.
6. J.I. Humadi, A.T. Nawaf, L.A. Khamees, Y.A. Abd-Alhussain, H.F. Muhsin, M.A. Ahmed, M.M. Ahmed, *Development of new effective activated carbon supported alkaline adsorbent used for removal phenolic compounds*, Commun. Sci. Technol. 8 (2023) 164–170.
7. Z. Mo, D.Z. Tai, H. Zhang, A. Shahab, *A comprehensive review on the adsorption of heavy metals by zeolite imidazole framework (ZIF-8) based nanocomposite in water*, Chem. Eng. J. 443 (2022) 136320.
8. O. Adi Saputra, S. Pujiasih, V. Nur Rizki, B. Nurhayati, E. Pramono, C. Purnawan, *Silylated-montmorillonite as co-adsorbent of chitosan composites for methylene blue dye removal in aqueous solution*, Commun. Sci. Technol. 5 (2020) 45–52.
9. D.R. Wicakso, A. Mirwan, E. Agustin, N.F. Nopembriani, I. Firdaus, M. Fadillah, *Potential of silica from water treatment sludge modified with chitosan for Pb(II) and color adsorption in sasirangan waste solution*, Commun. Sci. Technol. 7 (2022) 188–193.
10. J. Zhou, X. Zhou, K. Yang, Z. Cao, Z. Wang, C. Zhou, S.A. Baig, X. Xu, *Adsorption behavior and mechanism of arsenic on mesoporous silica modified by iron-manganese binary oxide (FeMnOx/SBA-15) from aqueous systems*, J. Hazard. Mater. 384 (2020) 121229.
11. S.C.W. Sakti, D. Siswanta, Nuryono, *Adsorption of Gold(III) on Ionic Imprinted Amino-Silica Hybrid Prepared from Rice Hull Ash*, Pure. App.l Chem. 85 (2013) 211–223.
12. S. Hastuti, Nuryono, A. Kuncaka, *L-Arginine-Modified Silica for Adsorption of Gold(III)*, Indones. J. Chem. 15 (2015) 108–115.
13. P. Shao, D. Liang, L. Yang, H. Shi, Z. Xiong, L. Ding, X. Yin, K. Zhang, X. Luo, *Evaluating the adsorptivity of organo-functionalized silica nanoparticles towards heavy metals: Quantitative comparison and mechanistic insight*, J. Hazard. Mater. 387 (2020) 121676.
14. A.M. Hassan, W.A. Wan Ibrahim, M.B. Bakar, M.M. Sanagi, Z.A. Sutirman, H.R. Nodeh, M.A. Mokhter, *New effective 3-aminopropyltrimethoxysilane functionalized magnetic sporopollenin-based silica coated graphene oxide adsorbent for removal of Pb(II) from aqueous environment*, J. Environ. Manage. 253 (2020) 109658.
15. H. Ghaforinejad, H. Mazaheri, A.H. Joshaghani, A. Marjani, *Study on novel modified large mesoporous silica FDU-12/polymer matrix nanocomposites for adsorption of Pb(II)*, PLoS. One 16 (2021) e0245583.
16. H. Wang, Y. Lin, Y. Li, A. Dolgormaa, H. Fang, L. Guo, J. Huang, J. Yang, *A Novel Magnetic Cd(II) Ion-Imprinted Polymer as a Selective Sorbent for the Removal of Cadmium Ions from Aqueous Solution*, J. Inorg. Organomet. Polym. Mater. 29 (2019) 1874–1885.
17 Z. Ren, X. Zhu, J. Du, D. Kong, N. Wang, Z. Wang, Q. Wang, W. Liu, Q. Li, Z. Zhou, *Facile and green preparation of novel adsorption materials by combining sol-gel with ion imprinting technology for selective removal of Cu(II) ions from aqueous solution*, Appl. Surf. Sci.

435 (2018) 574–584.

18. Buhani, Narsito, Nuryono, E. Sri Kunarti, Suharso, *Adsorption competition of Cu(II) ion in ionic pair and multi-metal solution by ionic imprinted amino-silica hybrid adsorbent*, Desalination Water Treat. 55 (2015) 1240–1252.
19. L. Fan, C. Luo, Z. Lv, F. Lu, H. Qiu, *Removal of Ag+ from Water Environment Using A Novel Magnetic Thiourea-Chitosan Imprinted Ag+*, J. Hazard . Mater. 194 (2011) 193–201.
20. M. Monier, D.A. Abdel-Latif, *Synthesis and Characterization of Ion-Imprinted Chelating Fibers Based on PET for Selective Removal of Hg2+*, Chem Eng J. 221 (2013) 452–460.
21. A. Afzal, S. Feroz, N. Iqbal, A. Mujahid, A. Rehman, *A Collaborative Effect of Imprinted Polymers and Au Nanoparticle on Bioanalogous Detection of Organic Vapors*, Sens. Actuators B. Chem. 231 (2016) 431–439.
22. M. Monier, D.A. Abdel-Latif, *Fabrication of Au(III) Ion-Imprinted Polymer Based on Thiol-Modified Chitosan*, Int. J. Biol. Macromol. 105 (2017) 777–787.
23. J. Dobrzyńska, M. Dąbrowska, R. Olchowski, R. Dobrowolski, *An ion-imprinted thiocyanato-functionalized mesoporous silica for preconcentration of gold(III) prior to its quantitation by slurry sampling graphite furnace AAS*, Microchim. Acta. 185 (2018).
24. Buhani, Narsito, Nuryono, E.S. Kunarti, *Production of metal ion imprinted polymer from mercapto-silica through sol-gel process as selective adsorbent of cadmium*, Desalination 251 (2010) 83–89.
25. T. Wirawan, G. Supriyanto, A. Soegianto, *Preparation of a new Cd(II)-imprinted polymer and its application to preconcentration and determination of cd(ii) ion from aqueous solution by SPE-FAAS*, Indones. J. Chem. 19 (2019) 97–105.
26. H.T. Fan, Y. Sun, Q. Tang, W.L. Li, T. Sun, *Selective adsorption of antimony(III) from aqueous solution by ion-imprinted organic-inorganic hybrid sorbent: Kinetics, isotherms and thermodynamics*, J. Taiwan Inst. Chem. Eng. 45 (2014) 2640–2648.
27. A.K. Priya, V. Yogeshwaran, S. Rajendran, T.K.A. Hoang, M. Soto-Moscoso, A.A. Ghfar, C. Bathula, *Investigation of mechanism of heavy metals (Cr6+, Pb2+& Zn2+) adsorption from aqueous medium using rice husk ash: Kinetic and thermodynamic approach*, Chemosphere 286 (2022) 131796.
28. Y. Niu, J. Yang, R. Qu, Y. Gao, N. Du, H. Chen, C. Sun, W. Wang, *Synthesis of Silica-Gel-Supported Sulfur-Capped PAMAM Dendrimers for Efficient Hg(II) Adsorption: Experimental and DFT Study*, Ind. Eng. Chem. Res. 55 (2016) 3679–3688.
29. Y. Niu, R. Qu, H. Chen, L. Mu, X. Liu, T. Wang, Y. Zhang, C. Sun, *Synthesis of silica gel supported salicylaldehyde modified PAMAM dendrimers for the effective removal of Hg(II) from aqueous solution*, J. Hazard. Mater. 278 (2014) 267–278.
30. Z. Chang, F. Li, X. Qi, B. Jiang, J. Kou, C. Sun, *Selective and efficient adsorption of Au (III) in aqueous solution by Zr-based metal-organic frameworks (MOFs): An unconventional way for gold recycling*, J. Hazard. Mater. 391 (2020) 122175.
31. El-Said AG, Badawy NA, Garamon SE, *Adsorption of Heavy Metal Ions from Aqueous Solutions onto Rice Husk Ash Low Cost Adsorbent*, J. Environ. Anal. Toxicol. 8 (2018) 1000543..
32. A. Negrea, S. Ronka, M. Ciopec, N. Duteanu, P. Negrea, M. Mihailescu, Kinetics, *Thermodynamics and Equilibrium Studies for Gold Recovery from Diluted Waste Solution*, Materials 2021, Vol. 14, Page 5325 14 (2021) 5325.
33. R. Liu, P. Liang, *Determination of Gold by Nanometer Titanium Dioxide Immobilized on Silica Gel Packed Microcolumn and Flame Atomic Absorption Spectrometry in Geological and Water Samples*, Anal. Chim. Acta. 604 (2007) 114–118.
34. C. Hang, B. Hu, Z. Jiang, N. Zhang, *Simultaneous On-Line Preconcentration and Determination of Trace Metals in Environmental Samples Using A Modified Nanometer-Sized Alumina Packed Micro-Column by Flow Injection Combined with ICP-OES*, Talanta 71 (2007) 1239–1245.
35. X. Gao, Y. Zhang, Y. Zhao, *Biosorption and Reduction of Au (III) to Gold Nanoparticles by Thiourea Modified Alginate*, Carbohydr . Polym. 159 (2017) 108–115.